

## ■ Biological Chemistry &amp; Chemical Biology

# Single molecule fluorescence reveals dimerization of myristoylated Src N-terminal region on supported lipid bilayers

Anabel-Lise Le Roux,<sup>[a, b]</sup> Bruno Castro,<sup>[c]</sup> Erik T. Garbacik,<sup>[c]</sup> Maria F. Garcia Parajo,<sup>[c, d]</sup> and Miquel Pons\*<sup>[a]</sup>

The proto-oncogene tyrosine-protein kinase Src is a key element of signaling cascades involved in the invasive and metastasis-forming capacity of cancer cells. While membrane tyrosine-kinase receptors are known to dimerize, Src is classified as a non-receptor kinase and assumed to remain always monomeric. Here we demonstrate the formation of stable dimers by the first domains of myristoylated Src previously shown to be sufficient for Src trafficking. Src dimers fused to green fluorescent protein (GFP) on supported lipid bilayers were identified using single-molecule photobleaching experiments. Competition with a protein containing only native Src domains without GFP confirms that dimerization is a previously overlooked intrinsic property of Src. Dimerization is concomitant to membrane binding by the myristoylated forms of Src and may constitute a new regulation layer for the Src oncogene.

Cell signaling is the process by which cells respond to external stimuli at the cell membrane. Receptor proteins, including tyrosine kinases, are integral membrane components that once activated by extracellular ligands form signaling competent dimers or higher oligomers.<sup>[1]</sup> On the intracellular side, non-receptor tyrosine kinases are key downstream mediators of cellular signal transduction.<sup>[2]</sup> Supramolecular assemblies of downstream effectors have been recently suggested to explain

properties such as threshold kinetics, signal amplification, or noise reduction.<sup>[3]</sup>

Src is a paradigmatic non-receptor kinase involved in signaling pathways related to cell migration, proliferation and survival.<sup>[4]</sup> It is also an oncologic target since overexpression and overactivation of Src have been associated to cancer progression and poor clinical prognosis.<sup>[5]</sup>

Structurally, Src consists of three folded domains (SH3, SH2, and kinase SH1), the disordered unique domain and a SH4 region myristoylated at the N-terminus (Figure 1 A).<sup>[6]</sup>

While transient interactions between Src molecules, leading to the mutual phosphorylation and persistent activation, are known to occur,<sup>[7]</sup> Src and other non-receptor kinases are believed to be monomeric proteins.<sup>[8]</sup> However, recent observations have challenged this idea.<sup>[9]</sup>

Here, we applied single molecule photobleaching approaches<sup>[10]</sup> to elucidate the stoichiometry of the myristoylated N-terminus of Src fused to the enhanced-green fluorescent protein (MyrUGFP, Figure 1B) embedded in supported lipid bilayers (SLBs). This form of Src has been shown to be sufficient for rapid exchange between late endosomes and the plasma membrane<sup>[11]</sup>. We conclusively demonstrate the formation of membrane-anchored dimers. Src dimers had not been described previously and open a novel insight in Src function with potentially important implications in terms of signaling localization and kinetics.

Supported lipid bilayers (SLBs) composed of dipalmitoyl-phosphatidyl-choline (DPPC), and dipalmitoyl-phosphatidyl-glycerol (DPPG) at a DPPC:DPPG ratio of 2:1 (doped with LissRhode PE to enable fluorescent imaging of the SLB) were formed on glass coverslips by deposition of 100-nm liposomes (See SI). The use of negatively charged lipids mimics the negative charge of the cell membrane. In previous experiments using surface plasmon resonance (SPR) it was shown that electrostatic interactions contribute to increase binding of Myr-SH4 containing proteins and the formation of persistent bound forms, associated to dimerization<sup>[9a]</sup>. Diluted solutions of MyrUGFP were incubated with SLBs for 30 minutes at 45°C and the excess protein was rinsed with cold buffer. To confirm that GFP is fully matured in the MyrUGFP construct, we measured the relative UV absorption at 488 and 280 nm (results not shown): we calculated the protein concentration independently at these two wavelengths and obtained similar values.

[a] Dr. A.-L. Le Roux, Prof. M. Pons

Biomolecular NMR Laboratory, Organic Chemistry Department, University of Barcelona, Baldiri Reixac 10–12, 08028 Barcelona, Spain. E-mail: mpons@ub.edu

[b] Dr. A.-L. Le Roux

Institute for Research in Biomedicine (IRB-Barcelona), The Barcelona Institute of Science and Technology, Baldiri Reixac 10–12, 08028 Barcelona, Spain.

[c] Dr. B. Castro, Dr. E. T. Garbacik, Prof. M. F. Garcia Parajo

ICFO- Institut de Ciències Fotoniques, The Barcelona Institute of Science and Technology, 08860 Castelldefels (Barcelona), Spain.

[d] Prof. M. F. Garcia Parajo

ICREA-Institució Catalana de Recerca i Estudis Avançats, 08010 Barcelona, Spain.

Supporting information for this article is available on the WWW under <http://dx.doi.org/10.1002/slct.201600117>.

© 2016 The Authors. Published by Wiley-VCH Verlag GmbH & Co. KGaA. This is an open access article under the terms of the Creative Commons Attribution-NonCommercial License, which permits use, distribution and reproduction in any medium, provided the original work is properly cited and is not used for commercial purposes.

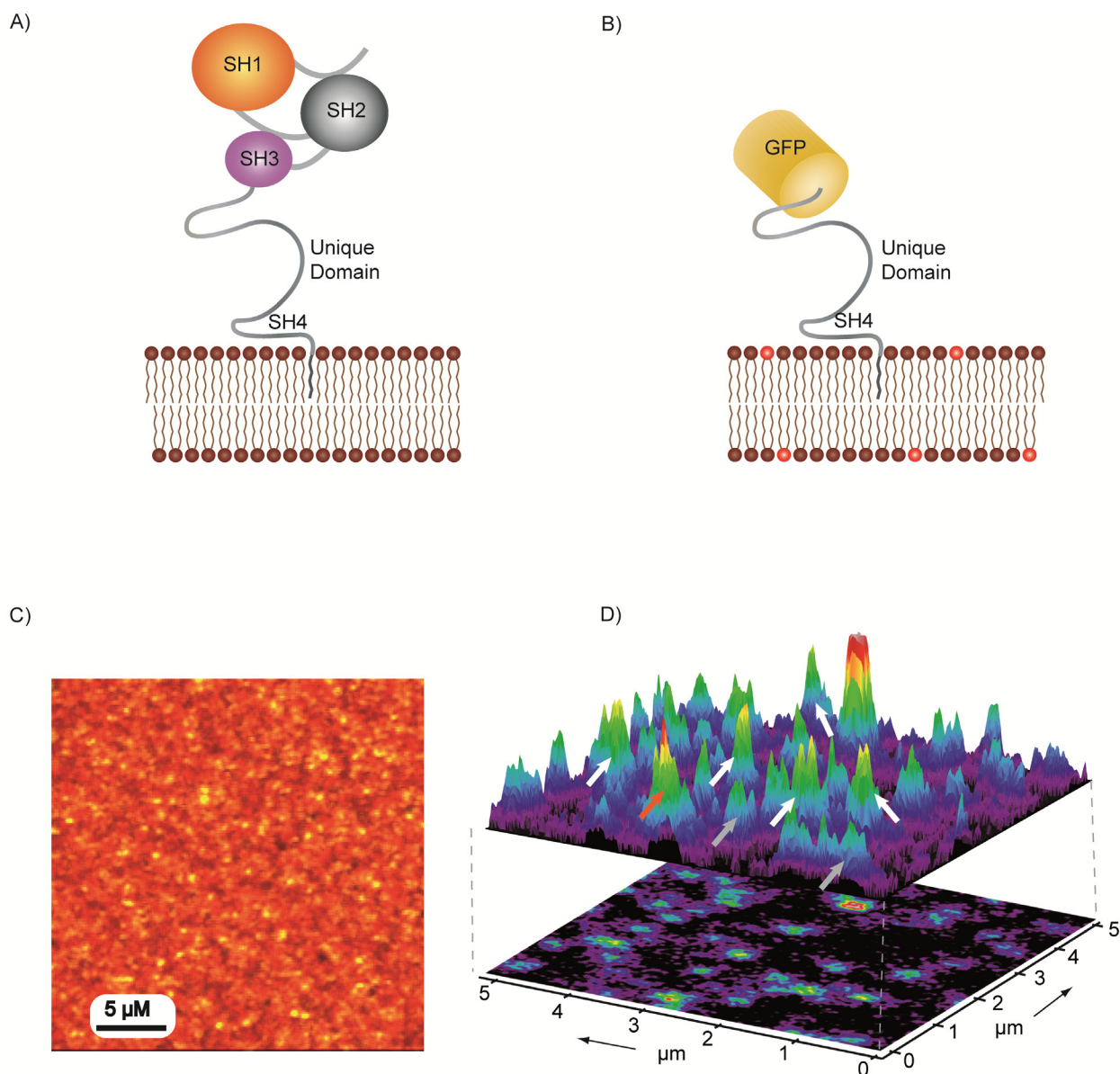


**Figure 1.** Schematic representation of A) native Src and B) MyrUGFP. C) Dual color confocal fluorescence image of the SLB (red) and MyrUGFP (yellow). D) Fluorescence intensity projection image of MyrUGFP bound to a deposited SLB, after protein incubation at 200pM.  $5 \times 5 \mu\text{m}^2$  area. The arrows highlight fluorescent spots with different intensities, low (grey), medium (white) and high (red).

The sample was imaged in buffer solution at room temperature, in which the lipid bilayer is in a gel phase, limiting protein lateral diffusion in the bilayer. However, previous SPR experiments showed that Src dimerization also occurs in liquid crystalline phases formed by dimyristoyl or dioleoyl phosphatidyl-choline.<sup>[9a]</sup> The detailed imaging conditions are described in the SI.

A representative two-color confocal fluorescence image of the SLB and bound proteins is shown in Figure 1C. A protein concentration of 200pM was chosen to guarantee single molecule discrimination under diffraction-limited confocal illumina-

tion. Individual, well-separated spots of GFP signal were readily identified, indicating the successful incorporation of MyrUGFP in the SLB. A projection of the fluorescence emitted by MyrUGFP is shown in Figure 1D. Fluorescence intensities varied significantly among individual fluorescent spots (e.g. compare the spots highlighted by colored arrows in Figure 1d), suggesting a distribution in the number of contributing chromophores. To quantify the number of proteins per spot, we generated individual fluorescence trajectories as a function of the observation time by positioning the fluorescence spots in the center of the excitation profile and recording the fluorescence

emission continuously for at least 20 seconds. Representative individual fluorescence trajectories are shown in Figure 2A–C. The trajectories showed the characteristic stepwise photobleaching behavior of single molecules and enabled the accurate quantification of the number of contributing chromophores.<sup>[10]</sup> A significant number of trajectories showed more than one single photobleaching step (Figure 2B,C).

We analyzed a large number of trajectories recorded at three different protein-incubation concentrations (200 pM, 500 pM and 750 pM), in which individual spots could be discriminated from the confocal images and classified them according to the number of bleaching steps (See SI). The experimental results are shown in Figure 2D. Remarkably, the majority of the trajectories showed the presence of two molecules at all the concentrations studied.

To investigate whether these results indeed reflect a dimerization of MyrUGFP on SLBs, or are the consequence of a high density of molecules randomly located at distances lower than the diffraction limit that could result in an apparent aggregation, we performed Monte Carlo simulations (see SI). For this, we considered the measured experimental molecular density at the different concentrations, and distributed the particles in a random fashion on a 2D matrix, after convolution with the point-spread function of the microscope. Simulations clearly show that in the absence of intermolecular binding interactions only a small fraction of the fluorescent spots should contain contributions from more than one molecule (Figure 2E). Therefore, the observation of a large fraction of spots with two or more fluorescent molecules demonstrates the formation of MyrUGFP dimers on SLBs.

We further performed a series of simulations assuming different ratios of monomers and dimers but also allowing for the presence of trimers. The complete results are shown in SI. Populations containing 20–30% of monomers and 80–70% of dimers reproduced best the experimental results in SLB (Figure 2F). At higher concentrations a slightly better agreement was found by adding a small fraction (5%) of trimers (Figure 2F). Overall, these data show that a large fraction of SLB-bound MyrUGFP molecules are dimers at all the concentrations studied.

To assess the role of the SLB in MyrUGFP dimerization, we deposited MyrUGFP directly on polylysine (PLL)-coated glass coverslips at a concentration rendering a comparable surface protein density to that of 500 pM protein on SLBs (Figure 3 A).

In the absence of SLBs, MyrUGFP was found mainly as monomers (~70%), with low percentages of dimers (28%) and trimers (3%), in good agreement with the values predicted by the simulations of non-interacting species (Figure 2E). These experiments also rule-out the dimerization of eGFP in solution prior to deposition on the substrate as a source for the MyrUGFP dimerization observed on SLBs. The absence of self-association of MyrUGFP in the concentration range between 1 nM and 10 μM (SI) was confirmed by the linear dependency of the fluorescence intensity with protein concentration. Non-myristoylated and myristoylated UGFP showed similar retention times by size exclusion chromatography suggesting they are both monomeric in solution (results not shown). Importantly, these data indicate that lipid binding is a requisite for MyrUGFP dimeriza-

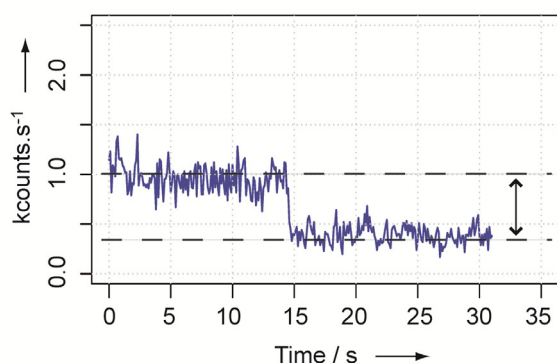
tion, probably associated to the confinement and restricted diffusion in the 2D membrane.

In order to confirm that dimerization was a property of the Src N-terminal domain we designed a competition experiment using MyrUSH3, a non-fluorescent protein containing the natural SH3 domain following the Unique domain. We compared fluorescence time traces recorded on SLBs incubated with a solution containing 200 pM of MyrUSH3 and 200 pM of MyrUGFP with respect to samples incubated under the same conditions but in the absence of MyrUSH3. The percentage of single photobleaching steps increased from ~15% to ~50% (Figure 3B). Consistently, the fraction of spots containing two fluorescent molecules decreased by 25% and those with three molecules by ~70%. These results can be explained by the formation of mixed dimers (MyrUSH3-MyrUGFP) with a single fluorophore, therefore giving rise to a single photobleaching step (Figure 3C). These results clearly indicate the formation of MyrUSH3-MyrUGFP mixed dimers, confirming that the interaction involves the N-terminal region of Src.

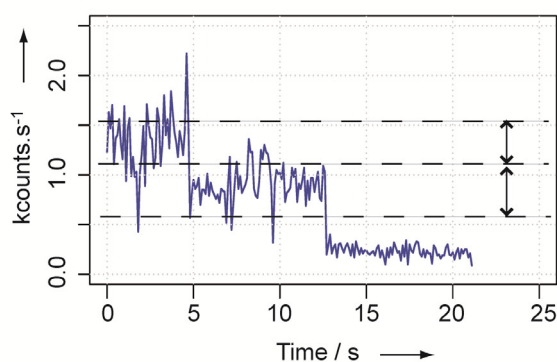
Our data are consistent with recent evidence of persistently lipid bound forms of MyrUSH3 with very slow dissociation kinetics. Binding of this form obeyed a second order rate law consistent with a dimerization process.<sup>[9a]</sup> The large proportion of dimers observed in the present experiments suggests that they are enriched in the SLB as the less tightly bound monomers are preferentially washed away. Other myristoylated species containing the Src SH4 domain show evidence of self-association upon membrane binding: MyrSH4 binds persistently to lipids<sup>[9a]</sup> and a SH4 peptide fused to a photo-switchable fluorescent protein show clusters by super-resolution imaging.<sup>[9b]</sup> Additionally, a <sup>2</sup>H-NMR study of d<sub>27</sub>-myristoylated SH4 inserted into lipid vesicles revealed unique structural and dynamic properties.<sup>[12]</sup> Thus, we postulate that MyrSH4 is the region directly involved in self-association, and we rule out that the SH3 or GFP domains participate in the dimerization. However, since MyrSH4 alone seems to form large oligomers, we suggest that the adjacent regions in Src probably have a role in restricting the oligomerization to the dimer/trimer level.

What are the possible biological implications of Src dimerization? Most other members of the Src family of kinases are strongly anchored to membranes by the simultaneous insertion of a myristic and a palmitic group. In contrast, Src has a single myristoyl chain, although complemented by electrostatic interactions.<sup>[6c]</sup> As a consequence, monomeric Src lipid binding is reversible. In contrast, Src dimers could bind much stronger to membranes by simultaneously inserting two myristoyl chains. The coexistence of Src monomers and dimers suggests that shifting the self-association equilibrium may modulate Src signaling. One can speculate that changes in local Src concentration or Src binding to receptors or co-receptors, among others, may favor Src dimerization, triggering persistent signaling from specific sites. The possibility that dimerization is an important component of the regulation and trafficking of Src is a novel and intriguing hypothesis that deserves further investigation.

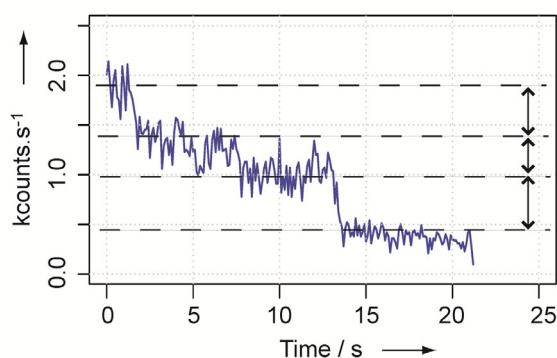
A) 1 molecule



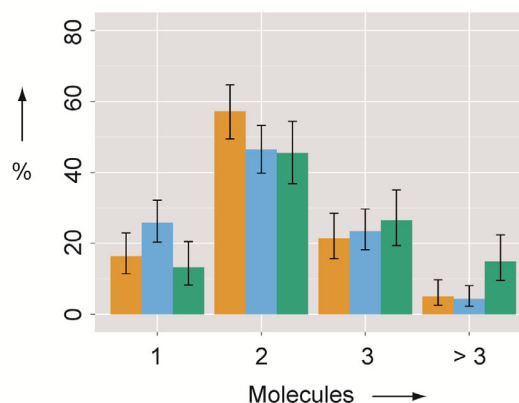
B) 2 molecules



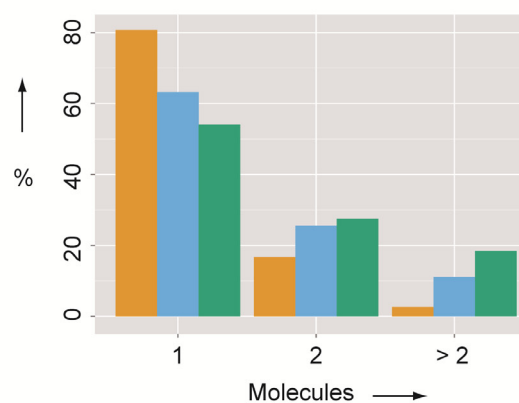
C) 3 molecules



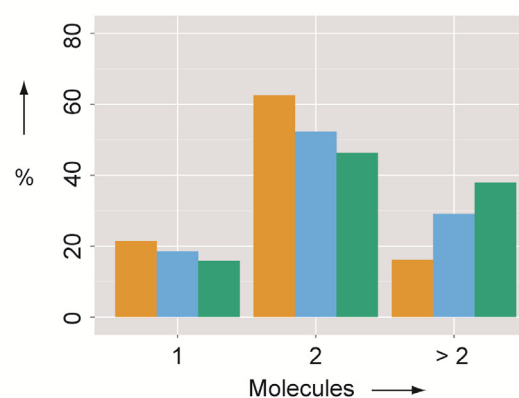
D) Experimental Data



E) Simulations\* 100:0:0



F) Simulations\* 25:70:5



200 pM    500 pM    750 pM

**Figure 2.** Fluorescence trajectories of MyrUGFP with A) one B) two and C) three discrete photobleaching steps. D) Distribution of the percentage of trajectories with one, two, three and more photobleaching steps at 200 pM ( $n = 159$ ), 500 pM ( $n = 220$ ), and 750 pM ( $n = 115$ );  $n$  is the number of trajectories. The error bars were extracted from a multimodal model fitting to the complete data set and correspond to the 95% confidence interval in the model (see SI for details). E-F) Predicted frequency distribution for a uniform population of non-interacting monomers E) or a mixed population containing a distribution of 25:70:5 of monomers, dimers, and trimers F). The total molecular density used in the simulations corresponded to the experimental data at each given concentration. Standard deviations of the numerical simulations were less than 2% in all cases and are not shown.

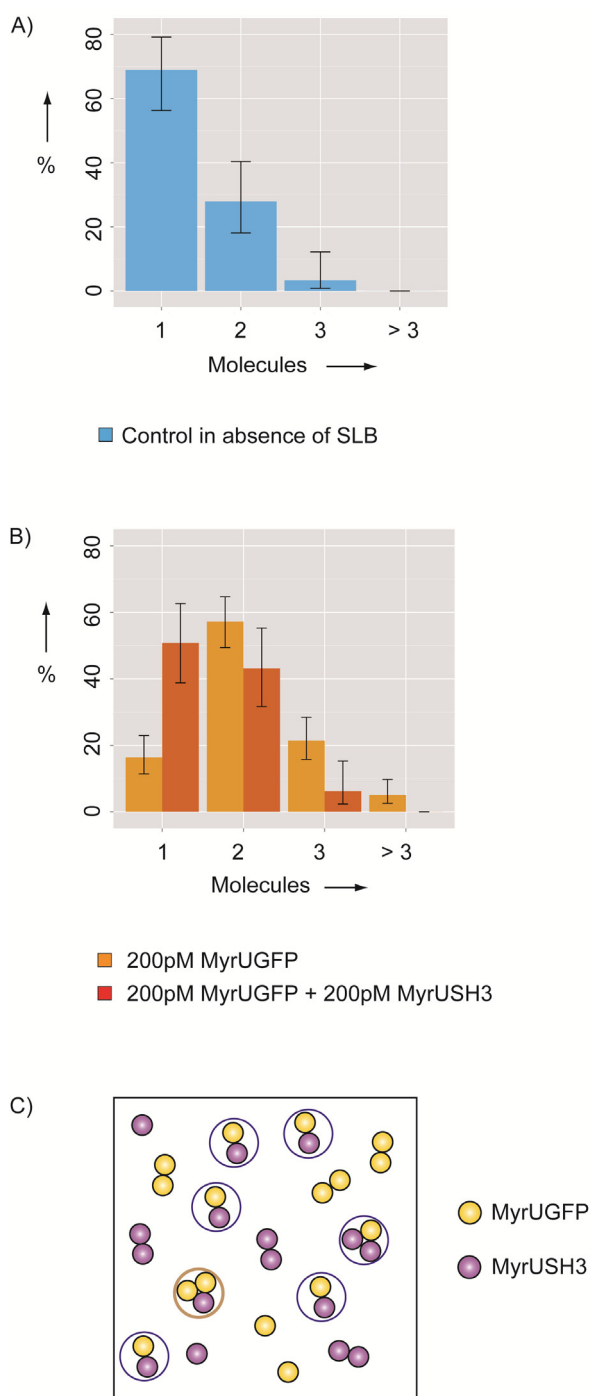


**Figure 3.** (a) Distribution of the percentage of trajectories with one, two, three and more photobleaching steps in MyrUGFP deposited on PLL-coated glass without SLB ( $n = 62$ ). The density is comparable to that of SLB samples incubated with 500 pM MyrUGFP. Error bars were computed as in Figure 2 (b) Comparison of the percentage of bleaching steps observed at the same concentration of MyrUGFP in the presence (red) and in the absence (orange) of non-fluorescent MyrUSH3 (64 trajectories). (c) Schematic representation of the competition experiment. Circles mark aggregates which display a lower number of photobleaching steps than the actual number of molecules.

## Supporting Information

The contents of the SI includes details of the constructs used, liposome and SLB preparation, fluorescence microscopy protocols, data processing and analysis, simulation protocols and extended simulation data, as well as control experiments in solution.

## Acknowledgments

This work was supported by funds from MINECO-FEDER (Spain) (BIO2013-45793-R), Fundació Marató TV3 and European Commission' 7<sup>th</sup> FP (GA 288263). ALR received a fellowship from IRB/La Caixa. BMC acknowledges the EC-Marie Curie COFUND action (ICFONEST). We thank Anna Lladó (IRB Microscopy Facility, Spain) for preliminary images, as well as Camille Otto (IRB Bio-statistics and Bioinformatics Unit, Spain) for help in data processing and analysis. We also thank Carlo Manzo (ICFO, Spain) for his contribution to simulations, Maria-Antonia Busquets (University of Barcelona, Spain) for her help in liposome preparation, and Mariano Maffei (BioNMR group) for help in the GFP-construct preparation.

**Keywords:** c-Src · Membrane-induced protein self-association · Non-receptor protein kinase dimers · Protein myristoylation · Single molecule photobleaching · Cell signaling,

- [1] a) H. E. Grecco, M. Schmick, P. I. Bastiaens, *Cell* **2011**, *144*, 897–909; b) J. T. Groves, J. Kuriyan, *Nature Struct. Mol. Biol.* **2010**, *17*, 659–665; c) M. Cebecauer, M. Spitaler, A. Sergé, A. I. Magee *J. Cell Sci.* **2010**, *123*, 309–320; d) S. R. Hubbard, W. T. Miller, *Curr. Opin. Cell Biol.* **2007**, *19*, 17–123.
- [2] a) M. A. Lemmon, J. Schlessinger, *Cell* **2010**, *141*, 1117–1134; b) J. S. Biscardi, R. C. Ishizawa, C. M. Silva, S. J. Parsons, *Breast Cancer Res.* **2000**, *2*, 203–210; c) J. Downward *Nature Rev. Cancer* **2003**, *3*, 11–22.
- [3] a) A. V. Hauenstein, L. Zhang, H. Wu *Curr. Opin. Struct. Biol.* **2015**, *31*, 75–83; b) H. Wu, *Cell* **2013**, *153*, 287–292.
- [4] a) D. J. Shields, D. Cheresch, c-Src. UCSD-Nature Molecule Pages **2014**, doi:10.1038/mp.a002227.01; b) M. C. Frame, *J. Cell Sci.* **2004**, *117*, 989–998; c) S.M. Thomas, J. S. Brugge, *Annu. Rev. Cell Dev. Biol.* **1997**, *13*, 513–609; d) S.J. Parsons, J. T. Parsons *Oncogene* **2004**, *23*, 7906–7909; e) R. Roskoski Jr, *Biochem. Biophys. Res. Commun.* **2004**, *324*, 1155–1164; f) E. Ingley, *Biochim. Biophys. Acta* **2008**, *1784*, 56–65.
- [5] a) T. J. Yeatman, *Nat. Rev. Cancer*, **2004**, *4*, 470–480; b) H. Alligayer, D. D. Boyd, M. M. Heiss, E. K. Abdalla, S. A. Curley, G. E. Gatlack, *Cancer* **2002**, *94*, 344–351.
- [6] a) P. Patwardhan, M. D. Resh, *Mol. Cell Biol.* **2010**, *30*, 4094–4107; b) C. Sigal, W. Zhou, C. A. Buser, S. McLaughlin, M. D. Resh, *Proc. Natl. Acad. Sci. USA* **1994**, *91*, 12253–12257; c) C. A. Buser, C. T. Sigal, M. D. Resh, S. McLaughlin, *Biochemistry* **1994**, *33*, 13093–13101.
- [7] a) G. Sun, L. Ramdas, W. Wang, J. Vinci, J. McMurray, R. J. A. Budde, *Arch. Biochem. Biophys.* **2002**, *397*, 11–17; b) E. Ingley, *Biochim. Biophys. Acta* **2008**, *1784*, 56–65.
- [8] a) F. Sicheri, J. Kuriyan, *Curr. Opin. Struct. Biol.* **1997**, *7*, 777–785; b) S. W. Cowan-Jacob, G. Fendrich, P. W. Manley, W. Jahnke, D. Fabbro, J. Liebetanz, T. Meyer, *Structure*, **2005**, *13*, 861–871; c) P. Bernadó, Y. Pérez, D. I. Svergun, M. Pons, *J. Mol. Biol.* **2008**, *376*, 492–505.
- [9] a) A.L. Le Roux, M.A. Busquets, F. Sagués, M. Pons, *Colloids Surf. B: Biointerfaces*, **2016**, *138*, 17–25; b) D.M. Owen, C. Rentero, J. Rossy, A. Magenau, D. Williamson, M. Rodriguez, K. Gaus, *J. Biophoton.* **2010**, *3*, 446–454.
- [10] a) M.F. Garcia-Parajo, M. Koopman, E. M. H. P. van Dijk, V. Subramaniam, N. F. van Hulst, *Proc. Natl. Acad. Sci. USA* **2001**, *98*, 14392–14397; b) M.F. Garcia-Parajo, G. M. J. Segers-Nolten, J. A. Veer-

- man, J. Greve, N. F. van Hulst, *Proc. Natl. Acad. Sci. U S A* **2000**, *97*, 7237–7242; c) N. Zijlstra, C. Blum, I. M. J. Segers-Nolten, M. M. A. E. Claessens, V. Subramaniam, *Angew. Chem. Int. Ed.* **2012**, *51*, 8821–8824.
- [11] K. Kasahara, Y. Nakayama, A. Kihara, D. Matsuda, K. Ikeda, T. Kuga, Y. Fukumoto, Y. Igarashi, N. Yamagushi, *Exp. Cell Res.* **2007**, *313*, 2651–2666.
- [12] H. A. Scheidt, D. Huster, *Biophys. J.* **2009**, *96*, 36663–3672.

Submitted: February 15, 2016

Accepted: February 23, 2016